(Received 7 April 2024, Accepted 8 July 2024, Scheduled 23 September 2024)

Obtaining Low Sidelobe Level and Reduced Complexity in Linear and Planar Antenna Arrays Using Thinned Subarrays

Ahmed Jameel Abdulqader[1], Jafar Ramadhan Mohammed[1,*], and Yessar E. Mohammed Ali[2]

[1] *College of Electronics Engineering, Ninevah University, Mosul 41002, Iraq*
[2] *Department of Computer and Communications Engineering, College of Engineering, Nawroz University, Duhok 42001, Iraq*

ABSTRACT: Conventionally, the thinning process in antenna arrays was performed at the element level with random selection after examining all the possible combinations. Thus, the computational time of such thinned methods was relatively high. Reducing the undesirable high computational time of great interest. In this paper, the thinning process is performed at subarray level rather than element level, thus, the computational time and array complexity were significantly reduced while minimizing the peak sidelobe level (PSLL). The optimization process consists of two steps where in the first step the array elements are portioned into a number of nonuniform ascending subarrays, while in the second step some of the least significant subarrays were turned off. Moreover, two schemes were used to portion the array elements. The first one is based on portioning all the array elements into ascending subarrays. This is known as fully nonuniform ascending subarray configuration since the entire array elements were portioned into smaller unequal groups. The second one is based on portioning only part of the elements located at the sides of the array, while leaving the central elements individually without any partition. This is known as partially nonuniform ascending subarray configuration. The genetic optimization algorithm is used to find out optimally which subarrays need to be thinned (or turned off) by setting their excitation amplitudes to zero. The simulation results for a total of 100 elements linear array illustrate that the PSLL, in the full subarray configuration, can be minimized to more than -33 dB by thinning 5 subarrays. The complexity reduction percentage was 72% before thinning, and it becomes 82% after thinning. On the other hand, the PSLL in the partial subarray configuration was reduced down to more than 30 dB by thinning 4 subarrays at each side of the array. In this case, the complexity reduction percentage was 52% before thinning, and it becomes 60% after thinning. The number of individual central-elements on both sides of the array was 26, and the number of subarrays on both sides of the array was 22. Furthermore, the idea of the thinned subarrays was successfully extended and applied to the two-dimensional planar arrays of 100×100 elements.

1. INTRODUCTION

Large antenna arrays with unit-amplitude excitation weighting possess many good radiation characteristics such as directive beam patterns and narrow beam widths. They also have some undesirable features such as high sidelobes. Conventionally, tapered-amplitude excitation weighting was used to reduce undesirable sidelobes. Consequently, a large number of transmitting/receiving (T/R) units are needed to built proper feeding and divider networks where each element needs independent T/R units, and each of these units consists of a digital variable attenuator and phase shifter which are expensive. Thus, the implementation of such tapered-amplitude excitation weighting is complex and costly. Their designs' computational times are also long. One common approach to reduce the array complexity is by using subarrays instead of its element counterpart [1, 2]. Surely, subarrays need lower number of T/R units by connecting the output of each of them into a single T/R unit, and thus a considerable reduction in the feeding system can be obtained. However, the array performance may be affected under such a subarray design [3, 4]. Therefore, there was always a tradeoff between array performance and its complexity [5]. Consequently, many researchers have suggested different types of subarrays to get acceptable compromise between these two factors [6–10]. It is worth to mention that this topic is still an active research line in the antenna array design community [11]. On the other hand, the formulation of subarrays can be either in regular portions or irregular ones. Usually regular subarrays are associated with emerged undesirable grating lobes, while the irregular subarrays are not. Thus, the irregular subarrays are more preferable than the regular ones.

The irregular subarray method which was used to portion and simplify the large antenna arrays can be further processed by turning off some of the least significant (or useless) subarrays. More importantly, the optimization process can be carried out on the level of subarray excitation weights calculation which is far lower than the level of the individual element excitation weights. Subarray weights can be optimized under specific user-defined constraints. Imposing such constraints on the resultant array radiation patterns leads the array synthesis process to nonlinear problem, which requires efficient global optimization techniques. Thus, various evolution algorithms, such as genetic algorithm (GA) [12–14], differential evolution (DE) [1], and particle swarm optimization (PSO) [15] have been used to solve this nonlinear problem. The sparse restric-

* Corresponding author: Jafar Ramadhan Mohammed (jafar.mohammed@uoninevah.edu.iq).

tions such as convex and compressed sensing were also used to solve this problem [16–18].

In this paper, first the ordinary linear arrays are portioned either fully or partially into a number of nonuniform ascending subarrays. In the fully nonuniform ascending subarray configuration, all the array elements are portioned into smaller irregular subarrays. Thus, the computational time and array complexity of such configuration can be greatly reduced, while its radiation features may be most distorted. On the other hand, the partially nonuniform ascending subarray configuration is based on portioning only part of the array elements that located at the sides of the array whereas the central elements remain individually intact. Thus, its computational time and complexity are compromised with respect to its radiation features. Next, to maintain the radiation features of these two configurations undistorted, some desired boundary constraints can be enforced on their array patterns to keep them within the required envelope. Note that the thinning process is performed at the subarray level rather than element level, thus, the computational time and array complexity can be significantly reduced while the peak sidelobe level (PSLL) is minimized. Then, genetic optimization algorithm is used to optimally find out the least significant subarrays that need to be thinned (or turned off) by setting their excitation amplitudes to zero while preserving the array performance. Finally, the proposed linear subarray configurations were successfully extended to large two-dimensional planar arrays.

2. THE PROPOSED THINNED SUBARRAY CONFIGURATIONS

In this section, the performance of the fully and partially nonuniform ascending subarrays are demonstrated under thinning process at the subarray level.

2.1. The Fully Non-uniform Ascending Subarray Configuration

Consider a linear array of N even radiating elements that are distributed uniformly with inter-element spacing equal to d along the x-axis. Its normalized far-field array factor, AF, can be written as

$$\mathrm{AF}\,(u) = \sum_{n=1}^{N/2} w_n \cos\left[\frac{2n-1}{2}\,kdu\right] \tag{1}$$

where w_n is the complex excitation coefficient of the nth element, while A_n and p_n represent the amplitude and phase of w_n; k is the wave number and equal to $2\pi/\lambda$; λ is the free space wavelength; d is the inter-element spacing between any two successive elements; $u = \sin(\theta)$, θ is the elevation angle of the main beam in the desired radiation pattern. Note that the array elements are distributed equally and symmetrically about the centre of the array, thus, only half of the array elements can be considered. To proceed with the fully nonuniform ascending subarray configuration (FNAS), all the array elements are portioned into a number of irregular subarrays equal to S, and the resultant far-field array factor can be written as

$$\mathrm{AF}\,(u)_{\mathrm{FNAST}} = \sum_{s=1}^{S/2} C_s\,|W_s| \sum_{n=1}^{N/2} \alpha_{sn}\,|w_n| \cos\left[\frac{2n-1}{2}\,kdu\right] \tag{2}$$

where α_{sn} is a binary vector that contains only ones and zeros as

$$\alpha_{sn} = \begin{cases} 1, & \text{if } n\text{th element is belong to } s\text{th subarray} \\ 0, & \text{otherwise} \end{cases} \tag{3}$$

where w_n and W_s represent the element distribution amplitudes and subarray distribution amplitudes at both element and subarray levels, respectively. The sub-vector C_s contains an optimized subset of random ones and zeros that will be used to decide which subarrays are in the active state (ON) or in the passive thinned state (OFF). To find the optimized values as well as the best combinations of α_{sn}, W_s, and C_s, a genetic optimization algorithm is used. More details on this optimization procedure can be found in [19]. To relax the optimization process with such a high number of the design variables, we used a two-step optimization process. In the first step, the element distribution amplitudes, $|w_n|$, of N elements array for $n = 1, 2, ..., N/2$ are first optimized under some desired boundary constraints that may be imposed on the radiation pattern to get a referenced fully optimized linear array with limited sidelobe level and beamwidth. Then, in the second step, each subset of the optimized element distribution amplitudes that belong to a specific active subarray, C_s, was averaged to get the optimized value of the subarray distribution amplitudes, W_s.

Generally, the optimized element distribution amplitudes, w_n, that responsible for generating low sidelobe patterns have the highest magnitudes at the array center and gradually decreases toward the array ends. Such envelope's variation should be preserved with the configured subarrays to maintain the sidelobe levels within desired limit. To do this, subarrays are formed in ascending order where the first one starts with two elements only, while the second one contains three elements and so on. After averaging the excitation amplitudes of the elements within each subarray, the resulting subarray distribution amplitudes, W_s, will best approximates the original distribution amplitudes at the element level, w_n. In other words, W_s represents the discretization form of the w_n. Finally, turning off some of the least significant subarrays may affect neither the array performance nor the sidelobe levels. The least significant subarray represents the one that has a quantized level equal or close to another one in the subarray distribution amplitudes. Fig. 1 shows the portioned subarrays in the FNAS with thinned subarrays that are highlighted with white color boxes. To maintain the overall array aperture unchanged and consequently the array beam width pattern, the first and last subarrays on each side of the array were excluded from the thinning process.

2.2. The Partially Nonuniform Ascending Subarray Configuration

In this configuration, the subarrays are formed from the outer elements of the original linear array such that the central elements are left individually without any partition. Fig. 2 shows the configuration of the partially nonuniform ascending subarrays with thinned subset elements.

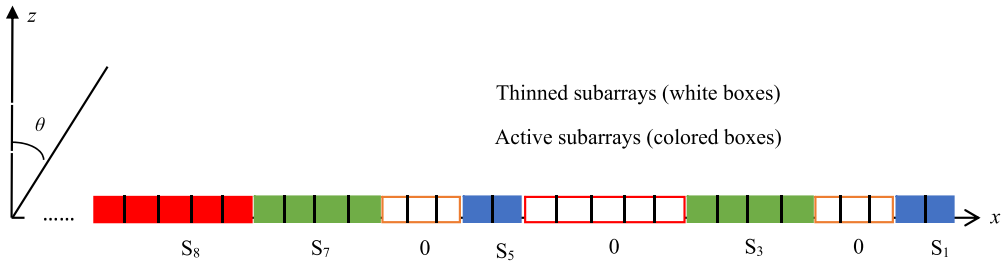

FIGURE 1. Right side of the subarray distributions using FNAST.

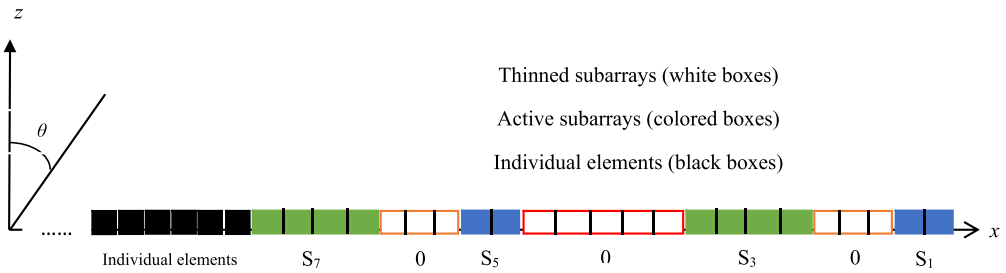

FIGURE 2. Right side of the subarray distributions using PNAST.

The main advantage of this configuration is its capability to provide a compromise tradeoff between array performance and array complexity. The normalized far-field array factor of this configuration can be written as:

$$\mathrm{AF}\,(u)_{\mathrm{PNAST}} = \sum_{m=1}^{M/2} H_m b_m \cos\left[\frac{2m-1}{2}\,kdu\right] + \sum_{s=1}^{S/2} C_s\,|W_s| \sum_{n=\frac{n-M+1}{2}}^{N/2} \alpha_{sn}\,|w_n| \cos\left[\frac{2n-1}{2}\,kdu\right] \tag{4}$$

where b_m is the nonoptimized unit-amplitude weighting distribution (i.e., $b_m = 1$ for $m = 1, 2, ..., M/2$) for all the central and individual elements, and H_m is a unity sub-vector that contains a set of one values to always activate the central individual elements.

For both configurations, the sidelobe level and beamwidth of their array patterns are controlled via the following user-defined boundary constraints (BCC)

$$\text{Cost function} \;=\; 20\mathrm{Log}_{10} \min \sum_{p=1}^{P} \left|\mathrm{AF}_{\mathrm{SC}}\,(u_p) - \mathrm{BCC}(u_p)\right|^2 \tag{5}$$

where $\mathrm{AF}_{\mathrm{SC}}$ is the array factor of subarray configurations either according to (1) for full subarray configuration or (2) for partial subarray configuration, and $p = 1, 2, ..., P$ are the examined sample points between these two patterns to get the minimum least-square difference between them. In other words, the cost function minimizes any excess magnitudes of the $\mathrm{AP}_{\mathrm{SC}}(u_p)$ located outside the user-defined constraint limits.

3. SIMULATION RESULTS

In order to demonstrate the effectiveness of both proposed configurations of fully and partially nonuniform ascending subarrays under thinned subset elements, several scenarios are tested. In all scenarios, the genetic algorithm is adopted in the optimization process under the following specifications: the number of populations was 30; the mutation rate was 0.16; and a single-point crossover selection was used. Moreover, the elements excitation amplitudes were only used in which their phases were set to zero. The total number of linear array elements is selected to be 100 (meaning that 50 elements on each side of the array will be portioned into proper subarrays). The number of elements in each formed subarray is arranged in an ascending order where the first subarray contains only two elements, then the second one contains three elements, and so on. Thus, the number of elements in each of the successive subarrays is $S = 2$, 3, 4, and 5. This pattern is repeated for the other parts of the array to cover the whole array aperture.

In the first scenario, all the radiating elements in the original linear array are divided into a set of subarrays arranged in ascending order according to the full subarray configuration method. After that, the least significant subarrays were thinned or turned off such that the array performance is not much affected. The complexity reduction (CR) percentage in the array feeding network can be calculated as:

$$\mathrm{CR}\% = \left[\frac{\text{Total number of subarrays} - \text{number of thinned subarrays}}{\text{Total number of array elements}}\right] \times 100\% \tag{6}$$

For $N = 100$ elements, a total number of 14 subarrays on each side of the array center were formed and arranged as in the fol-

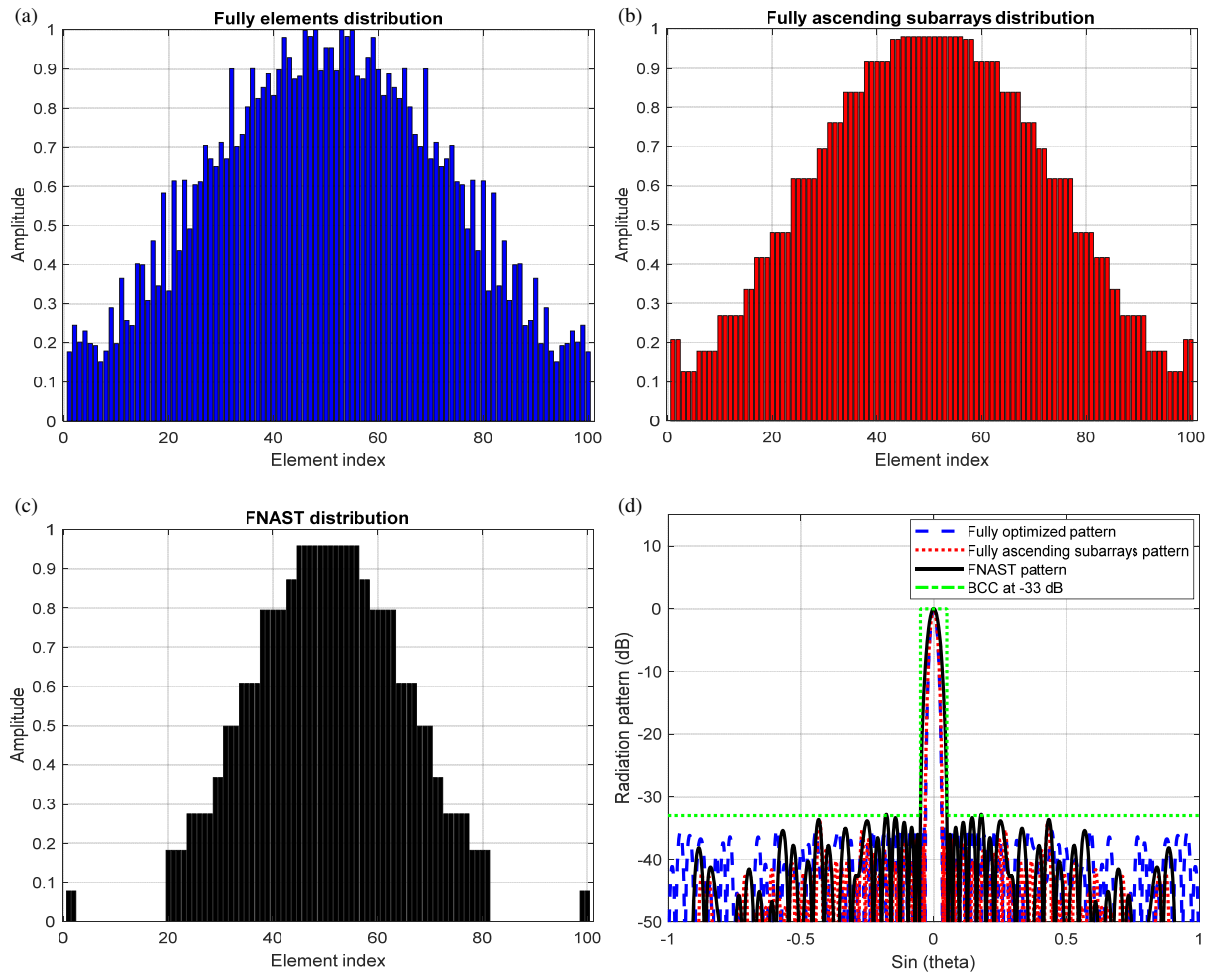

FIGURE 3. Results of the conventional fully optimized array at element level and the proposed full subarray configuration method with and without thinned subarrays. (a) Amplitude distribution of the fully optimized array at element level. (b) Amplitude distribution of the full subarrays without thinning. (c) Amplitude distribution of the full subarrays with thinning (FNAST). (d) Radiation patterns.

lowing vector: [2, 3, 4, 5, 2, 3, 4, 5, 2, 3, 4, 5, 2, 6]. Note that the subarray pattern [2, 3, 4, 5] was repeated three times, and the last two subarrays are chosen to have 2 and 6 elements, respectively. After applying the thinning process, some of these subarrays were turned off, and the result of the genetic optimization process was found as in the following vector: [2, 0, 0, 0, 0, 0, 4, 5, 2, 3, 4, 5, 2, 6]. Note that the locations of the thinned subarrays were randomly chosen according to the optimized C_s vector values. The complexity reduction percentage before applying the thinning subarrays was 72%, while after thinning subarrays it becomes 82%. Comparing this result with the thinning process at the element level, it is quite clear that the proposed thinned subarray is capable to provide better reduction in the array complexity while maintaining the array performance undistorted. It is worth to mention that such thinning percentage is not obtained in any other published work to the best of authors' knowledge. This extraordinary achievement is mainly due to thinned several subarrays instead of the element counterpart.

Figure 3 shows the results of applying the fully nonuniform ascending subarray configuration method with thinned subsets of elements (FNAST). To highlight its superiority and effectiveness, its performance has been compared to the same fully ascending subarrays pattern without thinned subset elements, and it has also been compared with the conventional fully optimized array pattern at the element level.

It is observed from this figure that the proposed fully nonuniform ascending subarray configuration method either with or without the thinned subset elements is capable to completely suppress the grating lobes which is a common feature with all existing regular subarray methods. It is also able to meet the user-defined boundary constraints (BCC) where the peak sidelobe level was kept below the desired limit of -30 dB. This approves the effectiveness of the proposed full subarray configuration method under thinned subset elements.

In the second scenario, the performance of the partially nonuniform ascending subarray configuration method was examined where the original N elements linear array was divided into two parts. The number of elements in the central array part is M, while in the other part it is $N - M$. The M elements in the first part are excited with unit-amplitude weighting, and they are left individually without partition. The $N - M$ elements in the second part are divided into subarrays. In this scenario, the value of M was set to 26 (i.e., 13 elements on

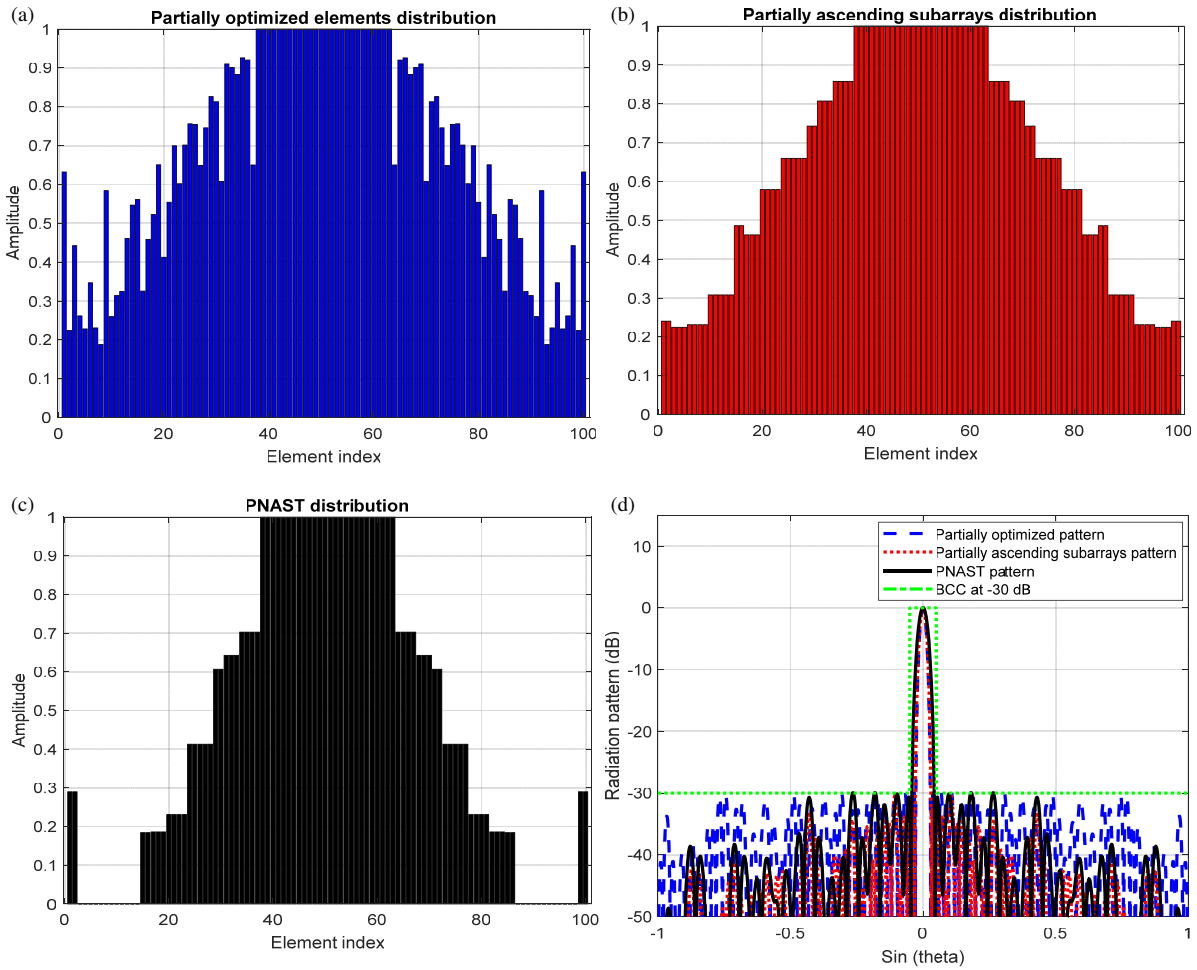

FIGURE 4. Results of the conventional partially optimized array at element level and proposed PNAST method with and without thinned subarrays. (a) Amplitude distribution of the partially optimized array at element level. (b) Amplitude distribution of the partially ascending subarrays without thinning. (c) Amplitude distribution of the partially ascending subarrays with thinning (PNAST). (d) Their radiation patterns.

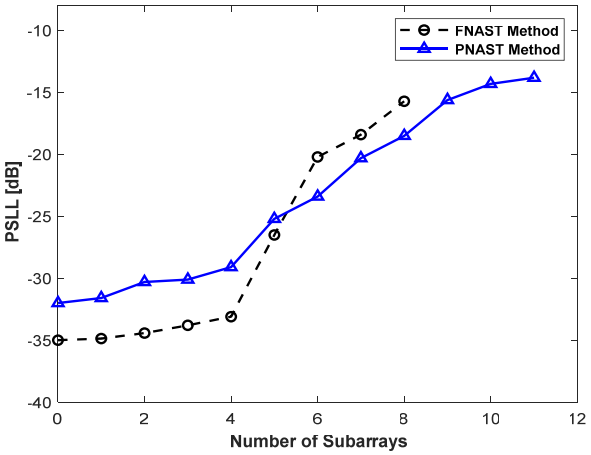

FIGURE 5. The PSLL versus number of subarrays.

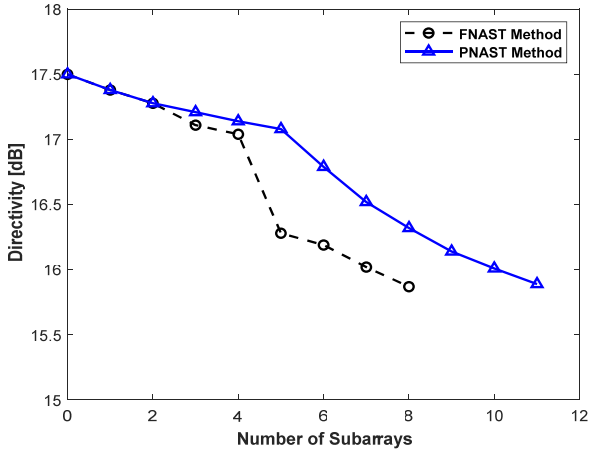

FIGURE 6. The directivity versus number of subarrays.

each side of the array center), while the number of elements in the second part of the array is 74 (i.e., 37 on each side of the array center) that are divided into 11 subarrays. The final division vector become as in follows: [2, 3, 4, 5, 2, 3, 4, 5, 2, 3, 4, 1, 1, 1, 1, 1, 1, 1, 1, 1, 1, 1, 1, 1], and after applying the thinning process, it results in [2, 0, 0, 0, 0, 3, 4, 5, 2, 3, 4, 1, 1, 1, 1, 1, 1, 1, 1, 1, 1, 1, 1, 1]. The complexity reduction percentage before applying the thinning process was 52%, and after thinning it became 60%. Fig. 4 shows the results of the optimized partially array pattern at the element level, proposed

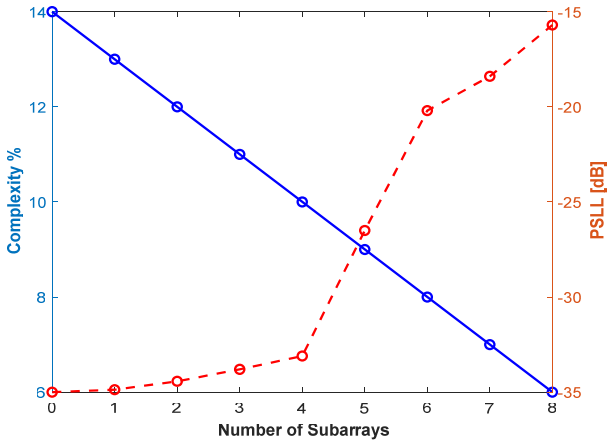

FIGURE 7. Complexity of FNAST versus number of subarrays.

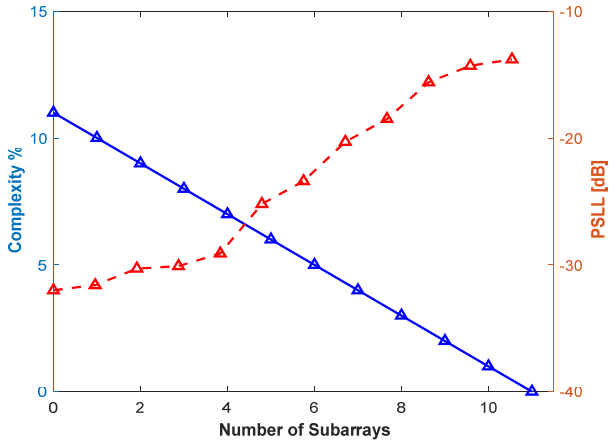

FIGURE 8. Complexity of PNAST versus number of subarrays.

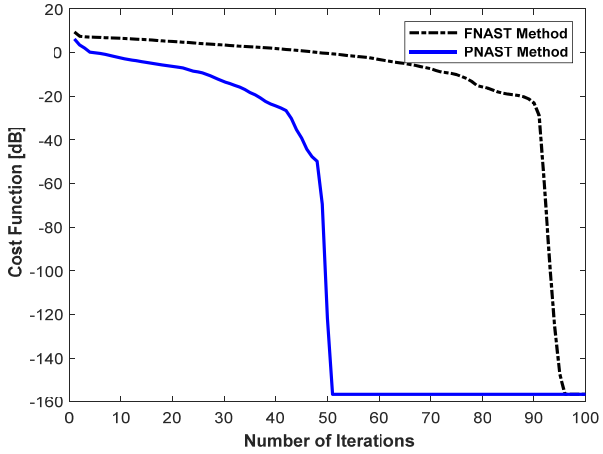

FIGURE 9. Cost functions of the FNAST and PNAST methods.

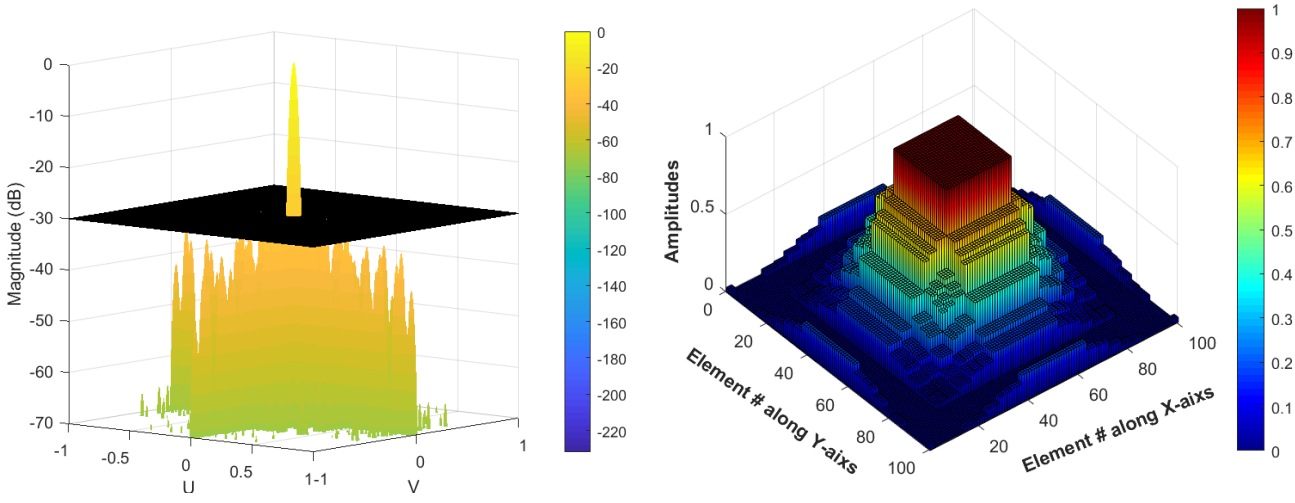

FIGURE 10. Results of 2D subarrays thinning with 100 × 100 elements.

partially subarray pattern without thinned subset elements, and the proposed partially nonuniform ascending subarray pattern with thinned subset elements (PNAST). Again, the proposed PNAST provides a good radiation pattern within the required user-defined boundary constraints (BCC).

In the next scenario, the performance of both proposed FNAST and PNAST configurations in terms of peak sidelobe level (PSLL), directivity (D), and the array complexity versus the number of subarrays are illustrated in Figs. 5, 6, 7, and 8, respectively. Generally, it can be seen that the PSLL and the di-

rectivity of both configurations increase with an increase in the number of subarrays, while the array complexity is reversed. However, the directivity is facing slight changes around 16 dB and 17 dB values due to the exception of the first and last subarrays from the thinning as mentioned earlier. By comparing between Figs. 7 and 8, it can be observed that any reduction in the complexity comes at the cost of higher sidelobe level. Also, it is noted that the complexity of the PNAST is lower than that of the FNAST due to the use of unity excitation for the central elements, thus, they are excluded from the complexity calculation. This gives an additional benefit to the PNAST method. Fig. 9 illustrates the cost function convergences of the FNAST and PNAST against the number of iterations. It is observed that the PNAST method needs approximately 50 iterations to converge, while the FNAST method requires more than 95 iterations. Thus, the computational time of the PNAST is shorter than that of the FNAST.

Finally, the partially subarray configuration method was extended to the large two-dimensional subarrays with size 100×100, and its array factor along with the corresponding subarray distribution amplitudes is shown in Fig. 10. From this figure, it is observed that the planar PNAST is capable to meet all the user-defined boundary constraints under thinned two-dimensional subset elements. The proposed two configurations can be used to simplify the massive MIMO systems while still guarantee good performances.

4. CONCLUSIONS

It is clear from the demonstrated results that the large linear and planar arrays can be effectively divided into smaller nonuniform ascending subarrays. Two different configurations based on the full and partial subarrays were suggested, and some of the least significant subarrays were thinned while preserving the array performance. Performing thinning process at the subarray level instead of the element level is a new idea, and it has not been previously discussed to the best of authors' knowledge. The peak sidelobe level (PSLL), in the fully nonuniform ascending subarray configuration was minimized to more than -33 dB by thinning 5 subarrays. The complexity reduction percentage was 86% before thinning, and it becomes 91% after thinning. The PSLL in the partially nonuniform ascending subarray configuration was reduced to more than -30 dB by thinning 4 subarrays at each side of the array. In this case, the complexity reduction percentage was only 89% before thinning, and it becomes 93% after thinning.

REFERENCES

[1] Jiang, H., Y. Gong, J. Zhang, and S. Dun, "Irregular modular subarrayed phased array tiling by algorithm X and differential evolution algorithm," *IEEE Antennas and Wireless Propagation Letters*, Vol. 22, No. 7, 1532–1536, Jul. 2023.

[2] Mohammed, J. R., "A novel linear and planar multiband fractal-shaped antenna arrays with low sidelobes," *International Journal of Communication Systems*, Vol. 37, No. 8, e5736, 2024.

[3] Haupt, R. L., "Optimized weighting of uniform subarrays of unequal sizes," *IEEE Transactions on Antennas and Propagation*, Vol. 55, No. 4, 1207–1210, Apr. 2007.

[4] Mohammed, J. R., "Minimizing grating lobes in large arrays using clustered amplitude tapers," *Progress In Electromagnetics Research C*, Vol. 120, 93–103, 2022.

[5] Mohammed, J. R., "Unconventional method for antenna array synthesizing based on ascending clustered rings," *Progress In Electromagnetics Research Letters*, Vol. 117, 69–73, 2024.

[6] Abdulqader, A. J., J. R. Mohammed, and R. H. Thaher, "Antenna pattern optimization via clustered arrays," *Progress In Electromagnetics Research M*, Vol. 95, 177–187, 2020.

[7] Brockett, T. J. and Y. Rahmat-Samii, "Subarray design diagnostics for the suppression of undesirable grating lobes," *IEEE Transactions on Antennas and Propagation*, Vol. 60, No. 3, 1373–1380, 2012.

[8] Abdulqader, A. J., J. R. Mohammed, and Y. A. Ali, "A T-shaped polyomino subarray design method for controlling sidelobe level," *Progress In Electromagnetics Research C*, Vol. 126, 243–251, 2022.

[9] El-Khamy, S. E., H. F. El-Sayed, and A. S. Eltrass, "New wideband antenna arrays with low sidelobe based on space filling curves," in *2023 International Microwave and Antenna Symposium (IMAS)*, 56–61, Cairo, Egypt, 2023.

[10] Abdulqader, A. J., J. R. Mohammed, and R. H. Thaher, "Phase-only nulling with limited number of controllable elements," *Progress In Electromagnetics Research C*, Vol. 99, 167–178, 2020.

[11] Anselmi, N., L. Tosi, P. Rocca, and A. Massa, "On the design of next generation phased array antennas — Methods, architectures, and trends," in *2023 17th European Conference on Antennas and Propagation (EuCAP)*, 1–4, Florence, Italy, 2023.

[12] Rocca, P., N. Anselmi, G. Oliveri, L. Poli, A. C. Stutts, and D. Erricolo, "Design of modular radar array antenna for two-way pattern sidelobe optimization," in *2022 IEEE Radar Conference (RadarConf22)*, 1–4, New York City, NY, USA, 2022.

[13] Mohammed, J. R., "Thinning a subset of selected elements for null steering using binary genetic algorithm," *Progress In Electromagnetics Research M*, Vol. 67, 147–155, 2018.

[14] Mohammed, J. R., "A method for thinning useless elements in the planar antenna arrays," *Progress In Electromagnetics Research Letters*, Vol. 97, 105–113, 2021.

[15] Zhang, Q. H., Q. H. Zhang, and Z. Y. Shen, "Planar array subarray division method in microwave wireless power transmission based on PSO&K-means algorithm," *IEEE Open Journal of Antennas and Propagation*, Vol. 4, 520–527, 2023.

[16] Abdelhay, M. A., N. O. Korany, and S. E. El-Khamy, "Synthesis of uniformly weighted sparse concentric ring arrays based on off-grid compressive sensing framework," *IEEE Antennas and Wireless Propagation Letters*, Vol. 20, No. 4, 448–452, 2021.

[17] Mohammed, J. R., R. H. Thaher, and A. J. Abdulqader, "Linear and planar array pattern nulling via compressed sensing," *Journal of Telecommunications and Information Technology*, Vol. 3, 50–55, Sep. 2021.

[18] Morabito, A. F., "Synthesis of maximum-efficiency beam arrays via convex programming and compressive sensing," *IEEE Antennas and Wireless Propagation Letters*, Vol. 16, 2404–2407, 2017.

[19] Mohammed, J. R., "Synthesizing non-uniformly excited antenna arrays using tiled subarray blocks," *Journal of Telecommunications and Information Technology*, Vol. 4, 25–29, Oct. 2023.